European Journal of Pharmaceutical Sciences 97 (2017) 70–78

Contents lists available at ScienceDirect

European Journal of Pharmaceutical Sciences

journal homepage: www.elsevier.com/locate/ejps

Pharmacokinetic/pharmacodynamic modeling of etoposide tumor growth inhibitory effect in Walker-256 tumor-bearing rat model using free intratumoral drug concentrations

Maiara Cássia Pigatto [a,b,c], Renatha Menti Roman [c], Letizia Carrara [d], Andréia Buffon [a,c], Paolo Magni [d], Teresa Dalla Costa [a,c,*]

[a] Pharmaceutical Sciences Graduate Program, College of Pharmacy, Federal University of Rio Grande do Sul, Porto Alegre, Brazil
[b] CAPES Foundation, Ministry of Education of Brazil, Brasília, DF, Brazil
[c] College of Pharmacy, Federal University of Rio Grande do Sul, Porto Alegre, Brazil
[d] Dipartimento di Ingegneria Industriale e dell'Informazione, University of Pavia, Italy

ARTICLE INFO

Article history:
Received 6 April 2016
Received in revised form 20 October 2016
Accepted 30 October 2016
Available online 02 November 2016

Keywords:
Etoposide
Pharmacokinetics/pharmacodynamics
Walker-256 tumor
Cancer chemotherapy
Tissue penetration
Mathematical model

ABSTRACT

The purpose of this study was to establish a population pharmacokinetic/pharmacodynamic (PK/PD) model linking etoposide free tumor and total plasma concentrations to the inhibition of solid tumor growth in rats. Walker-256 tumor cells were inoculated subcutaneously in the right flank of Wistar rats, which were randomly divided in control and two treated groups that received etoposide 5 or 10 mg/kg i.v. *bolus* every day for 8 and 4 days, respectively, and tumor volume was monitored daily for 30 days. The plasma and intratumoral concentrations-time profiles were obtained from a previous study and were modeled by a four-compartment population pharmacokinetic (popPK) model. PK/PD analysis was conducted using MONOLIX v.4.3.3 on average data and by mean of a nonlinear mixed-effect model. PK/PD data were analyzed using a modification of Simeoni Tumor Growth Inhibition (TGI) model by introduction of an E_{max} function to take into account the concentration dependency of $k_{2variable}$ parameter (variable potency). The Simeoni TGI-E_{max} model was capable to fit schedule-dependent antitumor effects using the tumor growth curves from the control and two different administered schedules. The PK/PD model was capable of describing the tumor growth inhibition using total plasma or free tumor concentrations, resulting in higher k_{2max} (maximal potency) for free concentrations (25.8 $mL \cdot \mu g^{-1} \cdot day^{-1}$ - intratumoral vs. 12.6 $mL \cdot \mu g^{-1} \cdot day^{-1}$ total plasma). These findings indicate that the plasma concentration may not be a good surrogate for pharmacologically active free tumor concentrations, emphasizing the importance of knowing drug tumor penetration to choose the best antitumor therapy.

1. Introduction

In the past decades, the application of pharmacokinetic/pharmacodynamic (PK/PD) modeling in the drug development process has increased substantially and has received more attention from the industry and regulatory agencies (Garnett et al., 2011; Gobburu, 2010; Jonsson et al., 2011). The PK/PD modeling using preclinical and clinical data has become a useful alternative for rational development of new drugs through early understanding of dose–response relationship and has enabled the optimization of dosing regimens for existing approved drugs, respectively (Bender et al., 2015; Friberg, 2003; Van Kesteren et al., 2003).

Because anticancer agents usually have a narrow therapeutic window, PK/PD models can be extremely useful in oncology guiding the selection of adequate doses that improve treatment efficacy and reduce toxicity (Mould et al., 2015). PK/PD models developed in oncology have been applied to describe the relation between drug plasma concentration and tumor growth (Ribba et al., 2012; Simeoni et al., 2004), biomarker response (Lindauer et al., 2010; Yamazaki et al., 2008), as well as adverse effects (Friberg et al., 2002; Quartino et al., 2012), using data from animals or humans.

The most usual PD marker in oncology is the tumor growth, where the measurements of the tumor volume are used to construct the time course of growth after administration of anticancer agents (Ribba et al., 2012; Rocchetti et al., 2005; Salphati et al., 2010; Simeoni et al., 2004). The most popular preclinical PK/PD model of tumor growth was developed by Simeoni et al. (2004). This model was primarily

Abbreviations: W256, Walker-256; HPLC-UV, high pressure liquid chromatography-ultraviolet; PK/PD, pharmacokinetic/pharmacodynamic; popPK, population pharmacokinetic; TGI, Tumor Growth Inhibition; NAD, Naïve Average Data; SAEM, stochastic approximation expectation maximization; GOF, goodness-of-fit; VPC, visual predictive check; AUC, area under the curve.

* Corresponding author at: Pharmaceutical Sciences Graduate Program, College of Pharmacy, Federal University of Rio Grande do Sul, Av. Ipiranga, 2752, Porto Alegre, RS 90.610-000, Brazil.
E-mail address: dalla.costa@ufrgs.br (T. Dalla Costa).

http://dx.doi.org/10.1016/j.ejps.2016.10.038
0928-0987/

developed for ranking competing preclinical candidates and was expanded to describe the tumor growth dynamics after administration of drug combinations (Terranova et al., 2013) as well as to predict suitable doses in humans from animal studies (Rocchetti et al., 2007).

The PK data most used to build the PK/PD model in pre-clinical and clinical oncology studies are the plasma concentrations assuming that these are a good surrogate for the drug concentrations reached in the tumor. Nevertheless, linking the effect to drug plasma concentrations can be misleading, since drug delivery into solid tumors is limited due to the heterogeneous microenvironment, with abnormal vascularization, hypoxic areas and high interstitial pressure characteristic of the tumor (Gallo, 2010; Grantab and Tannock, 2012; Wei et al., 2009; Zhou and Gallo, 2005). Drug plasma concentrations are commonly higher than those determined in the tumor as observed previously with epirubicin (Hunz et al., 2007), methotrexate (Sani et al., 2010) and reviewed by Fuso Nerini et al. (2014).

In this scenario, PK models that describe the concentrations in the tumor compartment can provide a better understanding of the drug distribution and drug efficacy helping to optimize dosing schedules. Up to date only a few PK/PD models have related anticancer tumor concentrations and effect, such as the model reported for temozolomide (Zhou et al., 2007), gefitinib (Sharma et al., 2013; Wang et al., 2008, 2009) and paclitaxel (Colin et al., 2014). Furthermore, these studies only investigated drug penetration into brain tumors, demonstrating the need for studies that consider the anticancer distribution to other types of solid tumors.

The anticancer agent etoposide is a topoisomerase II inhibitor used for treating hematopoietic malignancies and different solid tumors, such as small cell lung cancer, breast cancer and Kaposi's sarcoma. Although the systemic PK and PD of etoposide are extensively studied (Slevin, 1991; Toffoli et al., 2001), little is known about its distribution in solid tumors and PK/PD modeling linking its intratumoral concentrations with antitumor effect has not been reported.

In this context, the present study aims to comparatively model the PK/PD relationship between total plasma and free interstitial tumor etoposide concentrations to the tumor growth kinetics observed in a Walker-256 (W256) tumor-bearing Wistar rat model.

2. Materials and Methods

2.1. Chemicals and Reagents

Etoposide (purity ≥98%) and Trypan Blue solution 0.4% were purchased from Sigma-Aldrich (St. Louis, USA). Ethyl alcohol (anhydrous) and formic acid were purchased from Tedia (Fairfield, USA). Ultrapure water was obtained in a Millipore Milli-Q system (Bedford, USA). Polyethylene glycol (PEG) 300, polysorbate 80 and citric acid were acquired from Labsynth (São Paulo, Brazil). Glucose sterile solution was purchased from Basa (Caxias do Sul, Brazil). All other chemicals and reagents used in this study were of pharmaceutical or analytical grade.

Etoposide solution (5 mg/mL) was prepared for intravenous (IV) administration containing 3% citric acid 10%, 25% polyethylene glycol, 7.5% polysorbate 80, 10% ethanol (*v*/*v*) and the final volume was obtained with 5% glucose solution. This formulation is similar to the commercial injectable formulation used in humans (Kaul et al., 1995; Toffoli et al., 2001).

2.2. Animals and Tumor Model

Male Wistar rats (150–200 g) were supplied by the Center for Reproduction and Experimentation of Laboratory Animals (CREAL/UFRGS - Porto Alegre, Brazil) and received food and water ad libitum. Animal procedures were approved by UFRGS Ethical Committee on Animal Use (CEUA/UFRGS, protocol number 22302) and were conducted under standard conditions according Brazilian law (Brazil, 2008) and the guideline on experimental animal care and use (Brazil, 2013).

To obtain the tumor model, W256 carcinosarcoma cells were implanted intraperitoneally (IP) into Wistar rats (1×10^7 viable cells per animal). After 5–7 days of implantation, the ascitic tumor was harvested from the peritoneal cavity and the cell viability was evaluated by Trypan blue exclusion test (Phillips, 1973) using a Neubauer's chamber (Brand, Wertheim, Germany). To produce a solid tumor, 2×10^7 viable cells in 1 mL of phosphate-buffered solution were inoculated subcutaneously into the right flank of the animal. During harvesting and inoculation procedures the animals were anesthetized with a ketamine-xylazine (100–10 mg/kg). After inoculation, the animals were kept on separated in cages (4 rats/cage) in standard conditions of temperature, humidity and 12-h light–dark cycle during the period of treatment.

2.3. Pharmacokinetic Study

The pharmacokinetics of etoposide in W256 tumor-bearing Wistar rats was previously investigated in plasma and tumor (Pigatto et al., 2016). A population PK model (popPK) was developed using MONOLIX v. 4.3.3 (Lixoft, Orsay, France). The popPK model simultaneously described total etoposide concentrations in plasma and free concentrations in two regions of the tumor – center and periphery consisting of four-compartments with a saturable distribution into the tumor compartments and first-order elimination. The system of differential equations for the popPK model is given in Eq. 1:

$$\begin{aligned}
&\frac{dA(1)}{dt} = A(2)\cdot k_{21} + A(3)\cdot k_{31} + A(4)\cdot k_{41} - A(1)\cdot(k_{10}+k_{12}) - \left(\frac{V_{max}\cdot A(1)}{V_1\cdot k_m + A(1)}\right) - \left(\frac{V_{max}\cdot A(1)}{V_1\cdot k_m + A(1)}\right)\\
&\frac{dA(2)}{dt} = A(1)\cdot k_{12} - A(2)\cdot k_{21}\\
&\frac{dA(3)}{dt} = \left(\frac{V_{max}\cdot A(1)}{V_1\cdot k_m + A(1)}\right) - A(3)\cdot k_{31}\\
&\frac{dA(4)}{dt} = \left(\frac{V_{max}\cdot A(1)}{V_1\cdot k_m + A(1)}\right) - A(4)\cdot k_{41}\\
&C_{plasma} = \frac{A(1)}{V_1}\\
&C_{T.periphery} = \frac{A(3)}{V_3}\\
&C_{T.center} = \left(\frac{A(3)}{V_3}\cdot F_p\right) + \left(\frac{A(4)}{V_4}\cdot(1-F_p)\right)
\end{aligned} \tag{1}$$

A covariate model, in which the volume of plasma compartment V_1 is a function of the body weight, was used (Eq. 2):

$$V_{1i} = 0.171 \cdot \left(\frac{BW_i}{0.290}\right)^{0.581} \tag{2}$$

where V_{1i} is the volume of the central compartment for the i-th individual; 0.171 is the *(population)* volume of the central compartment estimated by the popPK model; 0.581 is the exponential scaling factor; BW is animal's individual body weight (kg); and 0.290 is the mean body weight (kg) in the PK group.

For the present PK/PD modeling, two sets of concentrations were used: total plasma concentration and free tissue concentration in the peripheral region of the tumor, because this region has a higher density of viable cancer cells that can be killed by the drug. Etoposide has a relatively short elimination half-life in tumor periphery ($\approx$2.39 h^{-1}) and in plasma ($\approx$1.83 h^{-1}), thus no accumulation was observed with the dose interval applied in the PD study. Total plasma and free peripheral tumor concentration-time profiles for the different treatments investigated in the PD experiments were simulated by fixing the following mean estimates values from the PK model previously described (Pigatto et al., 2016): elimination rate micro-constant from the central compartment (k_{10}) was 1.27 h^{-1}; the distribution rate micro-constants between compartments k_{12}, k_{21}, k_{31} and k_{41} were 2.86 h^{-1}, 2.88 h^{-1}, 3.99 h^{-1}, and 0.216 h^{-1}, respectively; the volume of the tumor periphery compartment (V_3) was 0.112 L; volume of the tumor center compartment V_4 was 2.99 L; maximum transporter velocity from the plasma to tumor (V_{max}) was 0.907 μg·h^{-1}; Michaelis-Menten constant

(k_m) was 5.15 μg/mL and the drug fraction (F_p) was 0.155. In the model it was assumed that the concentrations measured by microdialysis in the *center of the tumor represent* a mixed concentration of the real central concentration ($1 - F_p$) and the periphery concentration (F_p).

2.4. Pharmacodynamic Study

Five days after the tumor inoculation of the W256 carcinosarcoma cells into the animal right flank, when tumors had reached a palpable volume of 1 cm^3 in average, rats were selected and randomized into control and two treated groups and treatments started. IV *bolus* doses of etoposide were administrated to the two treated groups as following: 10 mg/kg once daily for 4 days ($n = 10$) or 5 mg/kg once daily for 8 days ($n = 11$). In order to maintain ceteris paribus condition, vehicle was administrated to the control group ($n = 10$).

Rats were clinically evaluated and weighted daily until 30 days after the inoculation time. Dimensions of the tumors were measured daily using a caliper and tumor mass was calculated as defined by Eq. 3 (Bueno et al., 2008; Simeoni et al., 2004):

$$Tumor\ \ weight\ \ (g) = \frac{length\,(cm) \cdot width^2\,(cm^2)}{2} \cdot \rho \tag{3}$$

assuming density $\rho = 1$ g/cm^3.

Rats with a tumor diameter higher than 4 cm, 20% weight loss and/or inability to eat and/or drink water were sacrificed before the end of the experiment according to the international guidelines for animal care and euthanasia (NCI, 2012).

2.5. Population Pharmacokinetic/Pharmacodynamic Model

To describe the tumor growth in response to etoposide dosing, the Simeoni TGI model (Simeoni et al., 2004) was used. This model consists of a system of ordinary differential equations, in which 5 parameters are used to describe the tumor growth. In particular, 3 parameters describe the tumor growth in absence of drug, while the 2 remaining parameters describe the drug action. Tumor growth in untreated animals (unperturbed growth model) showed by Eq. 4 is described by a growth function in which the exponential phase is followed by a linear one. In fact, when tumor weight reaches the threshold value $w_{threshold}$, the growth switch from exponential to linear because of nutrients limitation. The parameters λ_0 and λ_1, represent the rate of exponential and linear growth, respectively. The parameter w_0 is the tumor weight at the inoculation time and w(t) is the total tumor weight. ψ is a shape factor introduced to superimpose the continuity of the derivative and it is equal to 20 (Simeoni et al., 2004).

$$\begin{aligned} &\frac{dw}{dt} = \frac{\lambda_0 \cdot w(t)}{\left[1 + \left(\frac{\lambda_0}{\lambda_1} \cdot w(t)\right)^{\phi}\right]^{\frac{1}{\phi}}} \\ &w(0) = w_0 \end{aligned} \tag{4}$$

To describe the tumor growth in the treated animals (perturbed growth model), the previous growth function for untreated animals was modified by introducing a term to model the action of the cytotoxic agent as described in Eq. 5. In the Simeoni TGI model one assumes that, after drug administration, only a fraction of tumoral cells remains able to proliferate. In fact, cells hit by the drug stop proliferating and enter the transit compartmental system leading to cells death. This mortality chain represents the progressive degrees of damage that cells go through. The decreasing of proliferating cells is proportional both to the drug concentration (C(t)) and to the number of proliferating cells themselves. The parameter k_2 is the potency of anticancer compound, while k_1 is the first-order transfer rate constant describing the kinetic of cell death. In other words, it is related to how rapidly cells are brought to death. $Z_1(t)$ represents the mass of proliferating tumor cells, while $Z_2(t)$, $Z_3(t)$, $Z_4(t)$ are the mass of tumor cells in the different stages of damage (Simeoni et al., 2004).

$$\begin{aligned} &\frac{dZ_1(t)}{dt} = \frac{\lambda_0 \cdot Z_1(t)}{\left[1 + \left(\frac{\lambda_0}{\lambda_1} \cdot w(t)\right)^{\phi}\right]^{\frac{1}{\phi}}} - k_2 \cdot C(t) \cdot Z_1(t); \phi = 20 \\ &\frac{dZ_2(t)}{dt} = k_2 \cdot C(t) \cdot Z_1(t) - k_1 \cdot Z_2(t) \\ &\frac{dZ_3(t)}{dt} = k_1 \cdot Z_2(t) - k_1 \cdot Z_3(t) \quad Z_1(0) = w_0 \\ &\frac{dZ_4(t)}{dt} = k_1 \cdot Z_3(t) - k_1 \cdot Z_4(t) \quad Z_{2,3,4}(0) = 0 \\ &w(t) = Z_1(t) + Z_2(t) + Z_3(t) + Z_4(t) \end{aligned} \tag{5}$$

2.6. Data Analysis

Total plasma and free peripheral tumor concentration-time profiles of etoposide were obtained using the PK model previously developed (Pigatto et al., 2016) as described in 2.3. PD parameters were estimated performing a simultaneous fitting of the tumor growth curves observed both in control and treated animals.

PK/PD model was implemented using MONOLIX version 4.3.3. PD parameters were estimated using the stochastic approximation expectation maximization (SAEM) algorithm with log-likelihoods estimated by linearization and standard errors estimated by stochastic approximation.

A limit of quantification of 3 mm diameter corresponding to a 0.01 g was the minimum value that can be appreciate with the caliper. For the analysis, tumor measurements below the limit of quantification were coded as left censored data.

In this work, two different approaches were adopted: a pool approach using a Naïve Average Data (NAD) and a population approach. NAD is a very simple method that focuses the attention only on the typical population response. Average value of the data was computed for each sample time. Model was fitted against mean data. Contrariwise, with the population technique data from all the individuals involved in the study were taken into account. In this way, through a suitable mathematical model, it is possible to describe both typical subject data and variability among subjects.

Individual parameters P_i were supposed to be log-normally distributed. Random effects η_i were used to model inter-individual variability. They represent the random variation of the individual parameters around the population value θ (Eq. 6):

$$P_i = \theta \cdot \exp(\eta_i) \tag{6}$$

Random effects were normally distributed with zero mean and variance Ω, as it can be seen in the formula $\eta_i \sim N(0,\Omega)$. Different error models were tested for the residual unknown variability.

Fitting of predicted tumor growth curves against experimental data and precision estimates were the first criteria used to evaluate the adequacy of the model. Furthermore, it is important to underline that the first analysis was made using a NAD approach. Therefore, model was selected through the pool approach, and then implemented in a population context. The model evaluation was performed using goodness-of-fit plots (GOF) and visual predictive check (VPC), which is a common diagnostic tool that makes a comparison between statistics obtained from the simulated data using the estimated population parameters and the true observed data.

3. Results

The tumor growth inhibition and regrowth data from animals that received IV *bolus* administration of vehicle, etoposide 10 mg/kg-4 d

and 5 mg/kg-8 d are shown in Figs. 1, 2 and 3. The tumor growth curves showed a great difference between control and treated groups. Following international guidelines (NCI, 2012), the animals from the control group were sacrificed after 13.5 ± 2.5 d of tumor inoculation due to the size of the tumor. It was not possible to evaluate any animal until the end of experiment (30 days). The treated group that received etoposide 10 mg/kg-4d presented higher variability in the tumor regrowth; in average the animals were sacrificed after 27.2 ± 2.0 d of tumor inoculation, however 3 animals (Fig. 3 - numbers 4, 5 and 9) showed a slower tumor regrowth followed by regression in the last days of the experiment (data not shown). On the other hand, only 3 out of 11 animals were sacrificed 29 days after inoculation in the 5 mg/kg-8d group. The other animals were evaluated until the end of experiment.

The first modeling attempt employed the Simeoni TGI model described in the Materials and methods section using a pool approach, as illustrated in Fig. 1. One can observe that the model was not adequate to simultaneously describe the tumor growth in the control group and in the two treated groups, either considering etoposide plasma or tumor concentrations. The experimental regrowth curves showed that the 8-days treatment with 5 mg/kg/day presented greater tumor growth inhibition (regrowth observed after 21.4 ± 1.1 d) compared with 4-day treatment with 10 mg/kg/day (regrowth observed after 16.8 ± 0.8 d). These results indicate that etoposide has a schedule-dependent antitumor effect because the total drug dose used in each treatment (40 mg/kg) and the respective area under the curve (AUC) are the same for both regimens. When the PK/PD model uses tumor concentrations as the PK input (Fig. 1B), a slightly better fit can be observed because etoposide free concentrations at the site of action correlates better with effect than total plasma concentrations.

In fact, separate fitting of control and each treatment group (fitting not shown) estimated different values for the parameter k_2 using plasma concentrations (4.98 and 6.74 $mL \cdot \mu g^{-1} \cdot day^{-1}$ for 10 mg/kg-4 d and 5 mg/kg-8 d, respectively) or tumor concentrations (17.7 and 20.9 $mL \cdot \mu g^{-1} \cdot day^{-1}$ for 10 mg/kg-4 d and 5 mg/kg-8 d, respectively). These results indicate that etoposide potency differs between the two schedules, according to the terms definition of the model employed to fit the data. Either way, Simeoni TGI model was not adequate to simultaneously describe the effect of etoposide different schedules on the W256-tumor bearing rats.

Additionally, a total reduction of tumor volume (no measurable tumor) was observed between 11.6 ± 0.5 d and 16.8 ± 0.8 d for the 10 mg/kg-4 d treatment and between 12.1 ± 0.7 d and 21.4 ± 1.1 d for the 5 mg/kg-8 d treatment.

Viewing to improve data fitting it was assumed that k_2 in the Simeoni TGI model was variable and could be described by a inhibitory E_{max} function to takes into account its dependence on drug concentration (Eq. 7):

$$
\begin{aligned}
&k_{2variable} = k_{2\max}\left(1-\frac{C(t)}{IC_{50}+C(t)}\right)\\
&\frac{dZ_1(t)}{dt} = \frac{\lambda_0 \cdot Z_1(t)}{\left[1+\left(\frac{\lambda_0}{\lambda_1}\cdot w(t)\right)^{\varphi}\right]^{\frac{1}{\varphi}}} - k_{2variable}\cdot C(t)\cdot Z_1(t); \varphi = 20\\
&\frac{dZ_2(t)}{dt} = k_{2variable}\cdot C(t)\cdot Z_1(t) - k_1\cdot Z_2(t)\\
&\frac{dZ_3(t)}{dt} = k_1\cdot Z_2(t) - k_1\cdot Z_3(t) \quad Z_1(0) = w_0\\
&\frac{dZ_4(t)}{dt} = k_1\cdot Z_3(t) - k_1\cdot Z_4(t) \quad Z_{2,3,4}(0) = 0\\
&w(t) = Z_1(t) + Z_2(t) + Z_3(t) + Z_4(t)
\end{aligned}
\tag{7}
$$

This function was parameterized (I_{max}, assumed equal to 1) with IC_{50} that is the concentration that represents 50% of k_{2max} (the maximum drug potency). The new parameter $k_{2variable}$ was inserted into the Simeoni TGI model in place of k_2. According to the equations above, when drug concentration is close to zero (smaller than IC50): $k_{2variable}$ similar to k_{2max}. Instead, when concentration increases, the $k_{2variable}$ decreases. Note that, this modellization is equivalent to consider a saturable killing cell effect of the drug with the increases of its concentration, but it focuses the attention on the dug potency, one of the most import parameter of the Simeoni model. The mathematical relationship adopted in this paper is closed to that used in Rocchetti et al. (2013) to describe the interaction between an antiangiogenic and a cytotoxic drug. Through this equation, it is possible to explain the lower anticancer effect obtained when 10 mg/kg-4 d was administered to the animals in comparison with 5 mg/kg-8 d.

As observed in Fig. 2 (average data) and Fig. 3 (individual data), the Simeoni TGI-E_{max} model was able to simultaneously fit all control and the two treated groups. The model was able to provide a good description of the data both using total plasma (Figs. 2A and 3 – left panels) and free tumor concentrations (Figs. 2B and 3 – right panels).

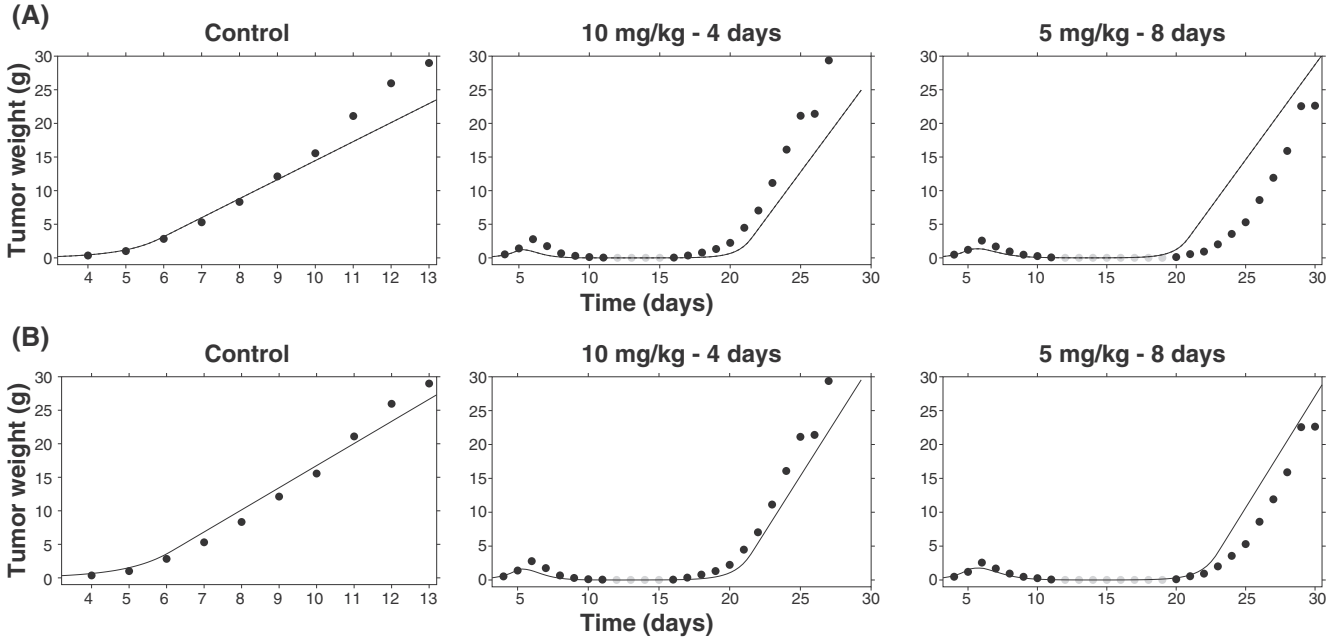

Fig. 1. Plots with average observed (black dots), left censored data (grey dots) and model-fitted (line) tumor growth curves in rats given either the vehicle (control) or etoposide i.v. (10 mg/kg for 4 days or 5 mg/kg for 8 days). Model predictions using the Simeoni TGI model considering total plasma (A – upper panels) and free tumor (B – lower panels) concentration.

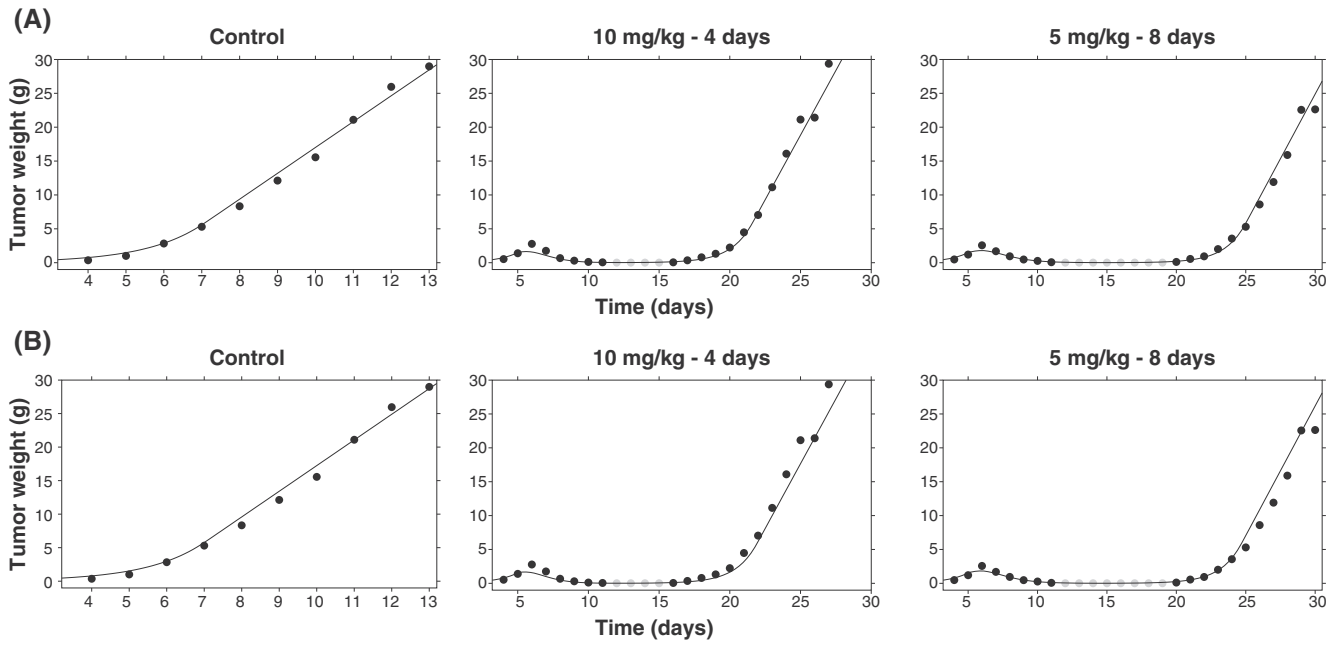

Fig. 2. Plots with average observed (black dots), left censored data (grey dots) and model-fitted (line) tumor growth curves in rats given either the vehicle (control) or etoposide i.v. (10 mg/kg for 4 days or 5 mg/kg for 8 days). Model predictions using the Simeoni TGI- E_{max} model considering total plasma (A – upper panels) or free tumor (B – lower panels) concentration.

The population parameter estimates are presented in Table 1, together with inter-individual and residual variability. Population parameters were identified with good precision (RSE ≤ 12%) and they were independent of the concentration used (plasma or tumor), except k_{2max}, which was of 12.6 $mL \cdot \mu g^{-1} \cdot day^{-1}$ when total plasma concentrations were used and 25.8 $mL \cdot \mu g^{-1} \cdot day^{-1}$ when free tumor concentrations were assumed. This difference is due to 82% lower tumor exposure to free etoposide than to total plasma concentrations. If free plasma concentrations were taken into account they would have been higher than the free concentrations determined in the tumor considering that etoposide plasma unbound fraction is about 30% and the tumor penetration factor in the periphery ($AUC_{0-t\ (tumor,\ free)}/AUC_{0-t(plasma,free)}$) is about 60%. Furthermore, etoposide tumor penetration was shown to be saturable, with $AUC_{tumor,free}$ does not increasing proportionally with the dose increase (Pigatto et al., 2016). Then, it makes no difference if free or total plasma concentrations are used, because both of them do not adequately reflect concentrations in target tissue. Accordingly to what previously was said, since the decrease in tumor cells growth rate is proportional to drug concentration via the proportional constant $k_{2variable,}$ the greater the concentration, the lower the potency of the compound.

Inter-individual variability was considered only for parameters related to the tumor growth w_0, λ_0 and λ_1. The inter-individual variability was moderate, ranging from 7.3 to 60.5% and it can be attributed to the differences in the tumor progression among the animals. Moreover, the variability estimated for tumor-related parameters could also be caused by the loss of some cells during the inoculation, determining differences in the growth curve between the animals. The inter-individual variability for the drug-related parameters (k_1, k_{2max} and IC_{50}) was not considered because it did not improve the fitting.

The error model chosen was a proportional plus power error model as follows (Eq. 8):

$$y = f + b \cdot f^c \cdot \varepsilon \tag{8}$$

where y is the data and f the model prediction. The coefficient of variation is expressed by b; c is fixed to 0.5; ε is the random variable to express the residual unknown variability, normally distributed with mean zero and variance 1. Residual variability was a bit high of 40% for both free tumor and total plasma concentrations.

GOF plots presented in Fig. 4 illustrate that the proposal PK/PD model adequately characterized etoposide antitumor effect. The individual and population predicted values are in good agreement with the observed tumor weights, using total plasma (Fig. 4A) or free tumor concentrations (Fig. 4B) as PK input in the model. Overestimation in the population predictions at higher tumor weights is caused by animals that presented a tumor growth slower than the others. For these animals it was possible to measure the dimension of the tumor until 19 days post-inoculation. For the others animals, especially for those belonging to the control group, measures were possible only until 13 days post-inoculation, because the tumor grew faster and these animals had to be sacrificed. Still in Fig. 4 it is possible to observe that the weighted residuals are randomly distributed around zero indicating the absence of model bias.

VPCs (Fig. 5) indicate that the final model effectively explained the observed tumor weights.

4. Discussion

In this study, we used the PK/PD modeling for describing tumor growth and the *anti*-tumor effect of etoposide in tumor-bearing rats. PK model was obtained from a previous work and linked to the PD model using total plasma or free peripheral tumor concentration-time profiles.

Modeling started using Simeoni TGI model already published, with the difference that besides plasma concentrations also the tumor concentrations of etoposide were employed to explain the cytotoxic effect of the drug. However, despite the flexibility of the Simeoni TGI model, it was not able to describe experimental data when all the groups were considered (control, 5 mg/kg/d-8 d, 10 mg/kg/d-4 d) either using plasma or tumor concentration as PK input.

As previously referred, in the Simeoni model the decreasing of the tumor growth rate caused by the drug is directly proportional to the number of proliferating tumor cells (Z_1) and the drug concentration via a proportionality constant k_2, which describes the potency of the drug. In the present study, however, this relation was not valid because it was observed that etoposide showed a schedule-dependent effect that resulted in a variable potency ($k_{2,variable}$).

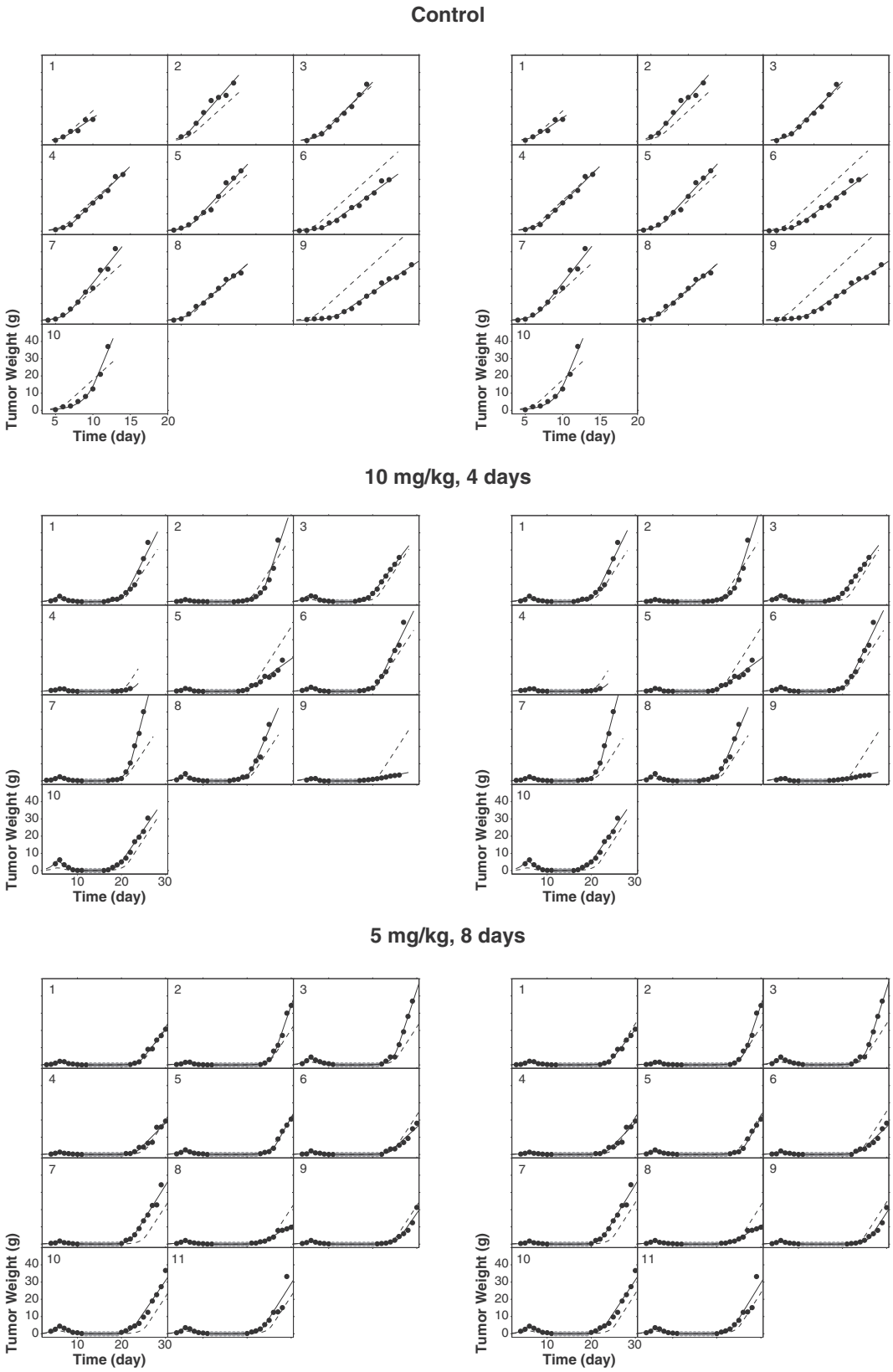

Fig. 3. Plots with observed (black dots), left censored data (grey dots), individual predicted (solid lines) and population predicted (dashed lines) tumor growth curves obtained in rats given either the vehicle (control) or etoposide i.v. (10 mg/kg-4 d or 5 mg/kg-8 d). In left panels total plasma concentrations were used, while in right panels free tumor concentrations were considered.

The dependence on schedule observed in this work corroborates previously studies that demonstrated that the etoposide response has been evidently schedule dependent (Dombernowsky and Nissen, 1973; Liu and Joel, 2003; Slevin et al., 1989) in clinical studies. Slevin et al. (1989) showed that patients with small-cell lung cancer receiving a 24-h infusion or the same dose divided over 5 days have positive

Table 1
Parameter estimates of the final PK/PD model.

Parameter	Estimate (RSE %)	
	Plasma[a]	*Tumor*[b]
Population mean		
λ_0 (day^{-1})	0.732 (2)	0.699 (2)
λ_1 ($g \cdot day^{-1}$)	3.91 (11)	4.00 (11)
w_0 (g)	0.037 (12)	0.043 (11)
k_1 (day^{-1})	1.63 (3)	1.62 (3)
k_{2max} ($mL \cdot \mu g^{-1} \cdot day^{-1}$)	12.6 (1)	25.8 (1)
IC_{50} ($\mu g \cdot mL^{-1}$)	1.07 (1)	1.08 (1)
Inter-individual variability		
ω (λ_0)	0.087 (20)	0.073 (20)
ω (λ_1)	0.605 (15)	0.595 (14)
ω (w_0)	0.554 (15)	0.555 (15)
Residual variability		
b and c	0.404 (4) and 0.5 fixed	0.403 (3) and 0.5 fixed
AIC	1223.93	1188.17

[a]Total plasma concentrations from the PK model; [b]free peripheral tumor concentrations from the PK model. Relative standard error = RSE % = (estimate/standard error) × 100; ω: standard deviation of inter-individual variability estimates; AIC: Akaike information criterion NA: not applicable. Model parameters are defined in the text.

response rates of 10% or 89%, respectively. Additionally, the schedule-dependent response of the epipodophyllotoxins such as etoposide (topoisomerase II inhibitor) has been related to the activity of topoisomerase II that it is variable during the cell cycle and also to the fast elimination of these drugs from the cell after the exposure, allowing cancer cells DNA repair. Accordingly, it is recommended in the literature the prolongation of the schedules of administration for these anticancer agents, using smaller daily doses, to improve the response (Hande, 1996; Joel and Slevin, 1994).

To model this schedule-dependent effect an inhibitory function was introduced in the Simeoni TGI model. Two new parameters were added - IC_{50} and k_{2max} - in order to describe the nonlinear relationship between concentration and effect. The rest of the model assumptions were similar to those originally presented for the Simeoni TGI model (Simeoni et al., 2004). The Simeoni TGI-E_{max} model successfully described etoposide effect on tumor growth using different dosing schedules. The population approach allowed to correctly describing the drug effect for the individual animals, estimating at the same time a typical value and the interindividual variability.

The same PK/PD model was used to describe the relationship between etoposide concentration and tumor growth inhibition using different PK input - free intratumoral interstitial concentrations or total plasma concentrations. The estimated k_{2max} was higher when free tumor concentrations were used, in accordance with the 82% lower drug exposure in tumor. This difference in k_{2max} (potency) depending on the PK input shows that total plasma concentration might not be a good surrogate for the pharmacologically active free tumor concentrations. When comparing antitumoral candidates using plasma concentrations as PK input, the PK/PD model can predict erroneous potency if the drugs have relevant differences in tumor penetration leading to inadequate selection of promising candidates.

The present study showed the development of a PK/PD model to correlate etoposide effect using either total plasma or free intratumoral concentrations allowing the investigation of the importance of PK input data on PK/PD modeling. Considering that PK/PD modeling is currently used in drug development, this study points out the importance of knowing free intratumoral drug behavior when building PK/PD models for antitumor drugs.

5. Conclusion

In this study, the population PK/PD Simeoni TGI-E_{max} model developed adequately described the schedule-dependent effect of etoposide using total plasma and free interstitial tumor etoposide concentrations obtained in a W256-tumor bearing Wistar rat model. The results suggested that the use of free intratumoral concentrations as PK input for PK/PD modeling could provide a better understanding of the pharmacokinetics and pharmacodymamics relationship shading light into the reasons for drug inefficacy that the traditional PK/PD models based on plasma concentrations are unable to supply.

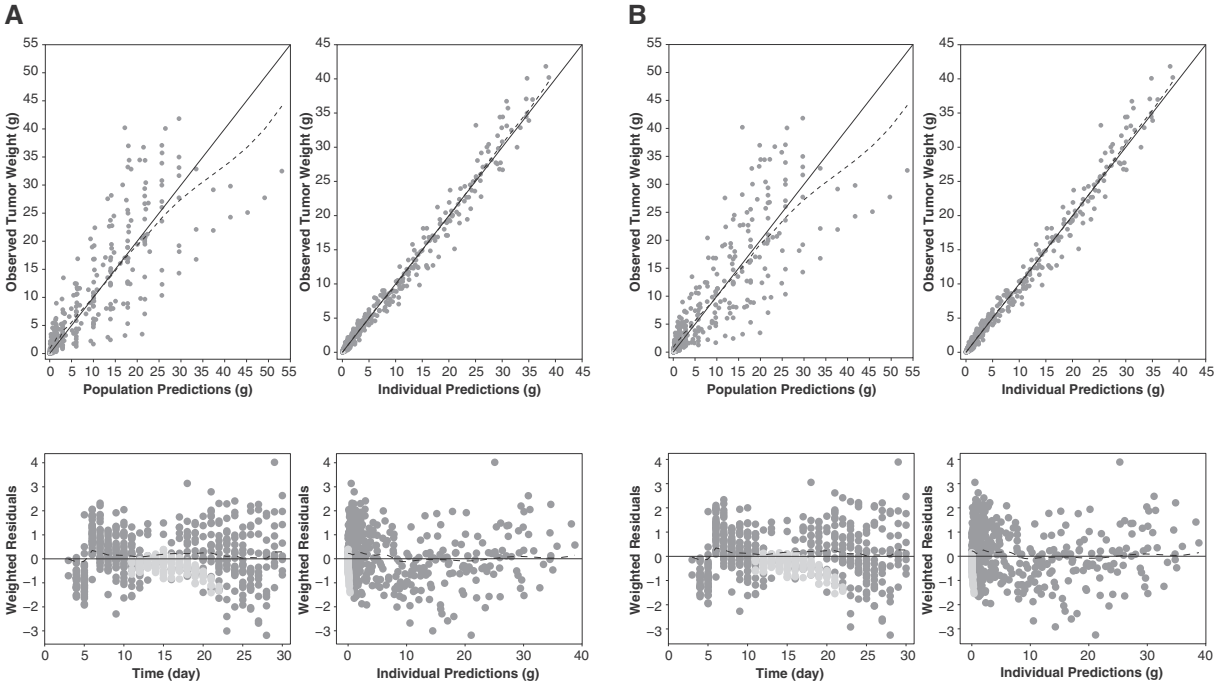

Fig. 4. Goodness-of-fit plots for the tumor weight using total plasma (A - four panels on the left side) or free tumor (B - four panels on the right side) concentrations. In the observed versus model predicted tumor weight plots (upper panels) the *solid* and *dashed lines* indicate the linear regression fit and identity line, respectively. In the panel below the residual plots are shown. The *grey dots* are the data, while the *light grey dots* represent the left censored data.

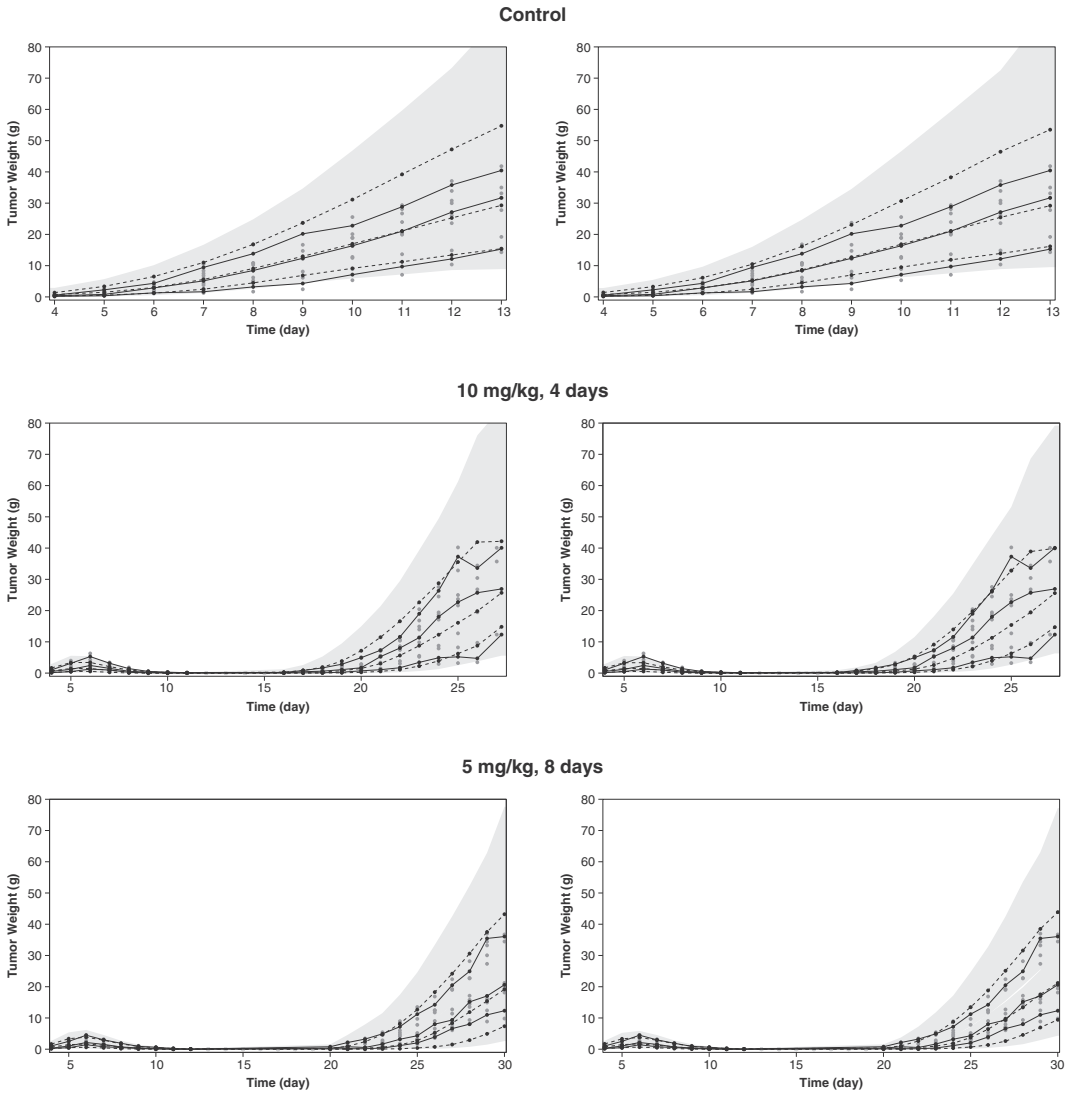

Fig. 5. VPC of the final PK/PD model stratified by group using total plasma (left panels) and free tumor (right panels) concentration based on 1000 simulated replicates of the original data. The *solid* and *dashed lines* show the 10th, 50th and 90th percentiles of observed and simulated data, respectively; the *grey shaded areas* represent the 90% confidence interval for the corresponding model predicted percentile. The left censored data are indicated by the *light grey dots*.

Acknowledgments

This work was supported by the National Counsel of Technological and Scientific Development (CNPq/Brazil) (project 477344/2011-9). Maiara Pigatto acknowledges CAPES Foundation/Brazil for PhD scholarship CAPES/Brazil and PDSE Program (Process #4929/14-4). The authors thank Dr. Sandra Coccuzzo Sampaio Vessoni from the Physiopathology Laboratory at Butantan Institute (São Paulo- SP, Brazil) who kindly donated the W-256 carcinosarcoma cells.

References

Bender, B.C., Schindler, E., Friberg, L.E., 2015. Population pharmacokinetic/pharmacodynamic modelling in oncology: a tool for predicting clinical response. Br. J. Clin. Pharmacol. 79 (1):56–71. http://dx.doi.org/10.1111/bcp.12258.

Brazil, 2008. Lei 11794/08: Procedimentos para Uso Científico de Animais. Diário Oficial da União, Seção 1 de 9 de outubro de 2008. Vol. CXLV (196), p. 1:2.

Brazil, 2013. Ministério da Ciência, Tecnologia e Inovação Conselho Nacional de Controle de Experimentação Animal – CONCEA. Diretriz Brasileira para o cuidado e a utilização de animais para fins científicos e didáticos – DBCA. Brasília-DF .

Bueno, L., de Alwis, D.P., Pitou, C., Yingling, J., Lahn, M., Glatt, S., Trocóniz, I.F., 2008. Semi-mechanistic modelling of the tumour growth inhibitory effects of LY2157299, a new type I receptor TGF-beta kinase antagonist, in mice. Eur. J. Cancer 44 (1):142–150. http://dx.doi.org/10.1016/j.ejca.2007.10.008.

Colin, P., De Smet, L., Vervaet, C., Remon, J.P., Ceelen, W., Van Bocxlaer, J., Boussery, K., Vermeulen, A., 2014. A model based analysis of IPEC dosing of paclitaxel in rats. Pharm. Res. 31 (10):2876–2886. http://dx.doi.org/10.1007/s11095-014-1384-5.

Dombernowsky, P., Nissen, N.I., 1973. Schedule dependency of the antileukemic activity of the podophyllotoxin-derivative VP 16-213 (NSC-141540) in L1210 leukemia. Acta Pathol. Microbiol. Scand. A. 81 (5):715–724. http://dx.doi.org/10.1111/j.1699-0463.1973.tb03564.x.

Friberg, L.E., 2003. Pharmacokinetic-pharmacodynamic modelling of anticancer drugs: haematological toxicity and tumour response in hollow fibres. (Doctoral thesis). Acta Universitatis Upsaliensis Uppsala.

Friberg, L.E., Henningsson, A., Maas, H., Nguyen, L., Karlsson, M.O., 2002. Model of chemotherapy-induced myelosuppression with parameter consistency across drugs. J. Clin. Oncol. 20 (24):4713–4721. http://dx.doi.org/10.1200/JCO.2002.02.140.

Fuso Nerini, I., Morosi, L., Zucchetti, M., Ballerini, A., Giavazzi, R., D'Incalci, M., 2014. Intratumor heterogeneity and its impact on drug distribution and sensitivity. Clin. Pharmacol. Ther. 96 (2):224–238. http://dx.doi.org/10.1038/clpt.2014.105.

Gallo, J.M., 2010. Pharmacokinetic/pharmacodynamic-driven drug development. Mt Sinai J. Med. 77 (4):381–388. http://dx.doi.org/10.1002/msj.20193.

Garnett, C.E., Lee, J.Y., Gobburu, J.V.S., 2011. Contribution of modeling and simulation in the regulatory review and decision-making: U.S. FDA perspective. In: Kimko, H.H.C., Peck, C.C. (Eds.), Clinical Trial Simulations, AAPS Advances in the Pharmaceutical Sciences 1. Vol. chapter 3, pp. 37–60.

Gobburu, J.V., 2010. Pharmacometrics 2020. J. Clin. Pharmacol. 50 (9):151S–157S. http://dx.doi.org/10.1177/0091270010376977.

Grantab, R.H., Tannock, I.F., 2012. Penetration of anticancer drugs through tumour tissue as a function of cellular packing density and interstitial fluid pressure and its modification by bortezomib. BMC Cancer 12:214. http://dx.doi.org/10.1186/1471-2407-12-214.

Hande, K.R., 1996. The importance of drug scheduling in cancer chemotherapy: etoposide as an example. Stem Cells 14 (1):18–24. http://dx.doi.org/10.1002/stem.140018.

Hunz, M., Jetter, A., Warm, M., Pantke, E., Tuscher, M., Hempel, G., Jaehde, U., Untch, M., Kurbacher, C., Fuhr, U., 2007. Plasma and tissue pharmacokinetics of epirubicin and paclitaxel in patients receiving neoadjuvant chemotherapy for locally advanced primary breast cancer. Clin. Pharmacol. Ther. 81 (5):659–668. http://dx.doi.org/10.1038/sj.clpt.6100067.

Joel, S.P., Slevin, M.L., 1994. Schedule-dependent topoisomerase II-inhibiting drugs. Cancer Chemother. Pharmacol. 34 (Suppl):S84–S88. http://dx.doi.org/10.1007/BF00684869.

Jonsson, S., Henningsson, A., Edholm, M., Salmonson, T., 2011. Contribution of modeling and simulation studies in the regulatory review: a European regulatory perspective. In: Kimko, H.H.C., Peck, C.C. (Eds.), Clinical Trial Simulations, AAPS Advances in the Pharmaceutical Sciences 1. Vol. chapter 2, pp. 15–36.

Kaul, S., Igwemezie, L.N., Stewart, D.J., Fields, S.Z., Kosty, M., Levithan, N., Bukowski, R., Gandara, D., Goss, G., O'Dwyer, P., 1995. Pharmacokinetics and bioequivalence of etoposide following intravenous administration of etoposide phosphate and etoposide in patients with solid tumors. J. Clin. Oncol. 13, 2835–2841.

Lindauer, A., Di Gion, P., Kanefendt, F., Tomalik-Scharte, D., Kinzig, M., Rodamer, M., Dodos, F., Sörgel, F., Fuhr, U., Jaehde, U., 2010. Pharmacokinetic/pharmacodynamic modeling of biomarker response to sunitinib in healthy volunteers. Clin. Pharmacol. Ther. 87:601–608. http://dx.doi.org/10.1038/clpt.2010.20.

Liu, W.M., Joel, S.P., 2003. The schedule-dependent effects of etoposide in leukaemic cell lines: a function of concentration and duration. Cancer Chemother. Pharmacol. 51 (4):291–296. http://dx.doi.org/10.1007/s00280-003-0579-y.

Mould, D., Walz, A.C., Lave, T., Gibbs, J.P., Frame, B., 2015. Developing exposure/response models for anticancer drug treatment: special considerations. CPT: Pharmacometrics Syst. Pharmacol. 4 (1), e00016. http://dx.doi.org/10.1002/psp4.16.

NCI, 2012. Frederick ACUC Guidelines Involving Experimental Neoplasia Proposals in Mice and Rats. (https://ncifrederick.cancer.gov/Lasp/Acuc/Frederick/Media/Documents/ACUC14.pdf (accessed 01.03.14)).

Phillips, H.J., 1973. Dye exclusions tests for cell viability. In: Kruse, J.R., Patterson, J.R.M.K. (Eds.), Tissue Culture, Methods and Applications. Academic Press, New York, pp. 406–408.

Pigatto, M.C., Araujo, B.V., Torres, B.G.S., Schmidt, S., Magni, P., Dalla Costa, T., 2016. Population pharmacokinetic modeling of etoposide free concentrations in solid tumor. Pharm. Res. 33:833–845. http://dx.doi.org/10.1007/s11095-016-1906-4.

Quartino, A.L., Friberg, L.E., Karlsson, M.O., 2012. A simultaneous analysis of the time-course of leukocytes and neutrophils following docetaxel administration using a semi-mechanistic myelosuppression model. Investig. New Drugs 30:833–845. http://dx.doi.org/10.1007/s10637-010-9603-3.

Ribba, B., Kaloshi, G., Peyre, M., Ricard, D., Calvez, V., Tod, M., Cajavec-Bernard, B., Idbaih, A., Psimaras, D., Dainese, L., Pallud, J., Cartalat-Carel, S., Delattre, J.Y., Honnorat, J., Grenier, E., Ducray, F., 2012. A tumor growth inhibition model for low-grade glioma treated with chemotherapy or radiotherapy. Clin. Cancer Res. 18 (18):5071–5080. http://dx.doi.org/10.1158/1078-0432.CCR-12-0084.

Rocchetti, M., Poggesi, I., Germani, M., Fiorentini, F., Pellizzoni, C., Zugnoni, P., Pesenti, E., Simeoni, M., De Nicolao, G., 2005. A pharmacokinetic-pharmacodynamic model for predicting tumour growth inhibition in mice: a useful tool in oncology drug development. Basic Clin. Pharmacol. Toxicol. 96 (3):265–268. http://dx.doi.org/10.1111/j.1742-7843.2005.pto960325.x.

Rocchetti, M., Simeoni, M., Pesenti, E., De Nicolao, G., Poggesi, I., 2007. Predicting the active doses in humans from animal studies: a novel approach in oncology. Eur. J. Cancer 43:1862–1868. http://dx.doi.org/10.1016/j.ejca.2007.05.011.

Rocchetti, M., Germani, M., Del Bene, F., Poggesi, I., Magni, P., Pesenti, E., De Nicolao, G., 2013. Predictive pharmacokinetic–pharmacodynamic modeling of tumor growth after administration of an *anti*-angiogenic agent, bevacizumab, as single-agent and combination therapy in tumor xenografts. Cancer Chemother. Pharmacol. 71 (5):1147–1157. http://dx.doi.org/10.1007/s00280-013-2107-z.

Salphati, L., Wong, H., Belvin, M., Bradford, D., Edgar, K.A., Prior, W.W., Sampath, D., Wallin, J.J., 2010. Pharmacokinetic-pharmacodynamic modeling of tumor growth inhibition and biomarker modulation by the novel phosphatidylinositol 3-kinase inhibitor GDC-0941. Drug Metab. Dispos. 38 (9):1436–1442. http://dx.doi.org/10.1124/dmd.110.032912.

Sani, S.N., Henry, K., Böhlke, M., Kim, J., Stricker-Krongrad, A., Maher, T.J., 2010. The effects of drug transporter inhibitors on the pharmacokinetics and tissue distribution of methotrexate in normal and tumor-bearing mice: a microdialysis study. Cancer Chemother. Pharmacol. 66:159–169. http://dx.doi.org/10.1007/s00280-009-1146-y.

Sharma, J., Lv, H., Gallo, J.M., 2013. Intratumoral modeling of gefitinib pharmacokinetics and pharmacodynamics in an orthotopic mouse model of glioblastoma. Cancer Res. 73 (16):5242–5252. http://dx.doi.org/10.1158/0008-5472.

Simeoni, M., Magni, P., Cammia, C., De Nicolao, G., Croci, V., Pesenti, E., Germani, M., Poggesi, I., Rocchetti, M., 2004. Predictive pharmacokinetic-pharmacodynamic modeling of tumor growth kinetics in xenograft models after administration of anticancer agents. Cancer Res. 64:1094–1101. http://dx.doi.org/10.1158/0008-5472.CAN-03-2524.

Slevin, M.L., 1991. The clinical pharmacology of etoposide. Cancer 67, 319–329 (DOI: 10.1002/1097-0142(19910101)67:1+<319::AID-CNCR2820671319>3.0.CO;2-D).

Slevin, M.L., Clark, P.I., Joel, S.P., Malik, S., Osborne, R.J., Gregory, W.M., Lowe, D.G., Reznek, R.H., Wrigley, P.F., 1989. A randomized trial to evaluate the effect of schedule on the activity of etoposide in small-cell lung cancer. J. Clin. Oncol. 7 (9), 1333–1340.

Terranova, N., Germani, M., Del Bene, F., Magni, P., 2013. A predictive pharmacokinetic–pharmacodynamic model of tumor growth kinetics in xenograft mice after administration of anticancer agents given in combination. Cancer Chemother. Pharmacol. 72 (2):471–482. http://dx.doi.org/10.1007/s00280-013-2208-8.

Toffoli, G., Corona, G., Sorio, R., Robieux, I., Basso, B., Colussi, A.M., Boiocchi, M., 2001. Population pharmacokinetics and pharmacodynamics of oral etoposide. Br. J. Clin. Pharmacol. 52 (5):511–519. http://dx.doi.org/10.1046/j.0306-5251.2001.01468.x.

Van Kesteren, C., Mathôt, R.A., Beijnen, J.H., Schellens, J.H., 2003. Pharmacokinetic-pharmacodynamic guided trial design in oncology. Investig. New Drugs 21 (2):225–241. http://dx.doi.org/10.1023/A:1023577514605.

Wang, S., Guo, P., Wang, X., Zhou, Q., Gallo, J.M., 2008. Preclinical pharmacokinetic/pharmacodynamic models of gefitinib and the design of equivalent dosing regimens in EGFR wild-type and mutant tumor models. Mol. Cancer Ther. 7 (2):407–417. http://dx.doi.org/10.1158/1535-7163.

Wang, S., Zhou, Q., Gallo, J.M., 2009. Demonstration of the equivalent pharmacokinetic/pharmacodynamic dosing strategy in a multiple-dose study of gefitinib. Mol. Cancer Ther. 8 (6):1438–1447. http://dx.doi.org/10.1158/1535-7163.MCT-09-0089.

Wei, Y.H., Xu, L.Z., Shen, Q., Li, F.Z., 2009. Microdialysis: a technique for pharmacokinetic-pharmacodynamic studies of oncological drugs. Curr. Pharm. Biotechnol. 10 (6):631–640. http://dx.doi.org/10.2174/138920109789069288.

Yamazaki, S., Skaptason, J., Romero, D., Lee, J.H., Zou, H.Y., Christensen, J.G., Koup, J.R., Smith, B.J., Koudriakova, T., 2008. Pharmacokinetic-pharmacodynamic modeling of biomarker response and tumor growth inhibition to an orally available cMet kinase inhibitor in human tumor xenograft mouse models. Drug Metab. Dispos. 36 (7):1267–1274. http://dx.doi.org/10.1124/dmd.107.019711.

Zhou, Q., Gallo, J.M., 2005. In vivo microdialysis for PK and PD studies of anticancer drugs. AAPS J. 7 (3):E659–E667. http://dx.doi.org/10.1208/aapsj070366.

Zhou, Q., Guo, P., Wang, X., Nuthalapati, S., Gallo, J.M., 2007. Preclinical pharmacokinetic and pharmacodynamic evaluation of metronomic and conventional temozolomide dosing regimens. J. Pharmacol. Exp. Ther. 321 (1):265–275. http://dx.doi.org/10.1124/jpet.106.118265.